Electronic Supplementary Material (ESI) for CrystEngComm.
This journal is © The Royal Society of Chemistry 2022

Electronic Supplementary Information (ESI)

The Effect of Ionic Liquids on the Nucleation and Growth of Perylene Films Obtained by Vapor Deposition

José C. S. Costa,*[a] Ricardo M. Campos,[a] Ângela C. M. Castro,[a] Artur F. M. Farinha,[a] Gonçalo N. P. Oliveira,[b] João P. Araújo,[b] Luís M. N. B. F. Santos[a]

[a] *CIQUP, Institute of Molecular Sciences (IMS), Department of Chemistry and Biochemistry, Faculty of Science, University of Porto, Portugal.*
**E-mail: jose.costa@fc.up.pt*
[b] *IFIMUP, Institute of Physics for Advanced Materials, Nanotechnology and Photonics, University of Porto, Portugal.*

Index

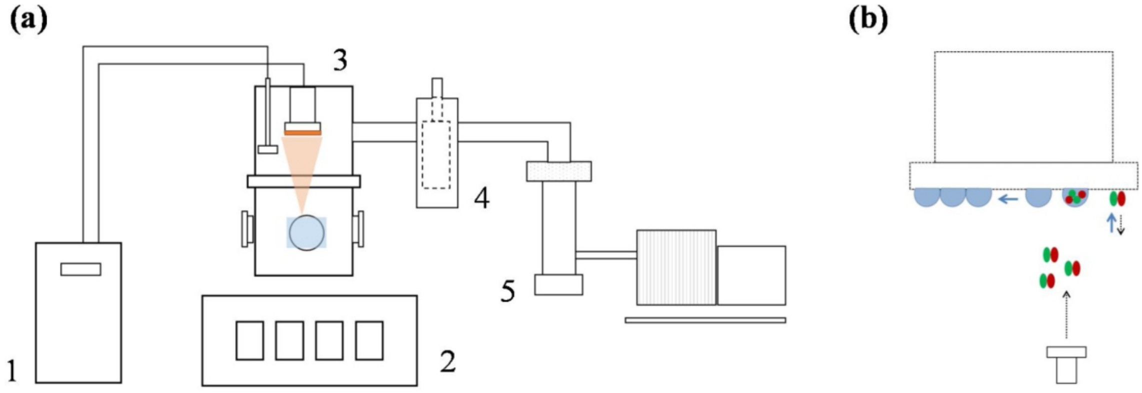

Fig. S1. Schematic representation of the physical vapor deposition (PVD) technique: (a) ThinFilmVD apparatus (1 – cooling system, 2 – instrumentation box, 3 – vacuum chamber, 4 – N_2 (l) metallic trap, 5 – vacuum pumping system); (b) schematic detail of the PVD/vacuum thermal evaporation process of ionic liquids. More details: *Appl. Surf. Sci.*, 2018, 428, 242 and *J. Chem. Eng. Data*, 2015, 60, 3776.

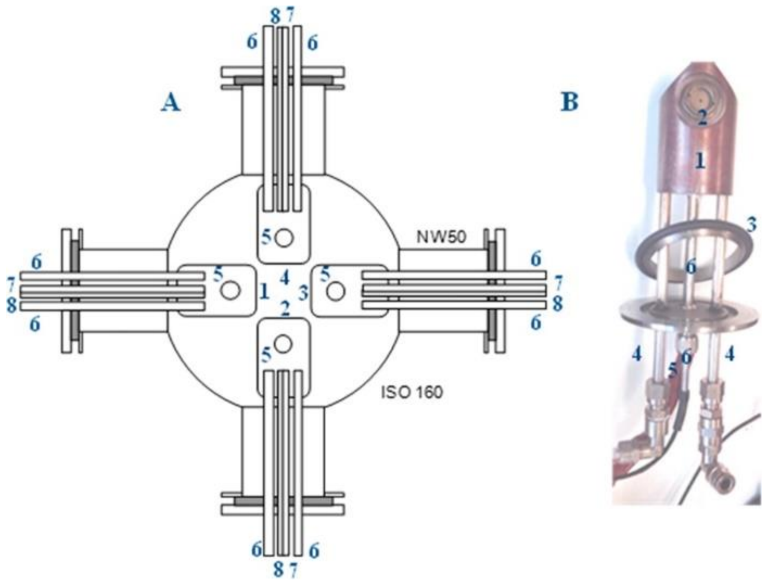

Fig. S2. A – Schematic representation of the ovens: 1, 2, 3, 4 – individual ovens; 5 – cavity of the Knudsen cell screwing; 6 – air cooling tube; 7 – heater; 8, – Pt100 sensor; B – Image of an individual oven (top view): 1 – copper block; 2 – Knudsen cell; 3 – Viton O-ring; 4 – cooling system; 5 – heater; 6 – Pt100. More details: *J. Chem. Eng. Data*, 2015, 60, 3776.

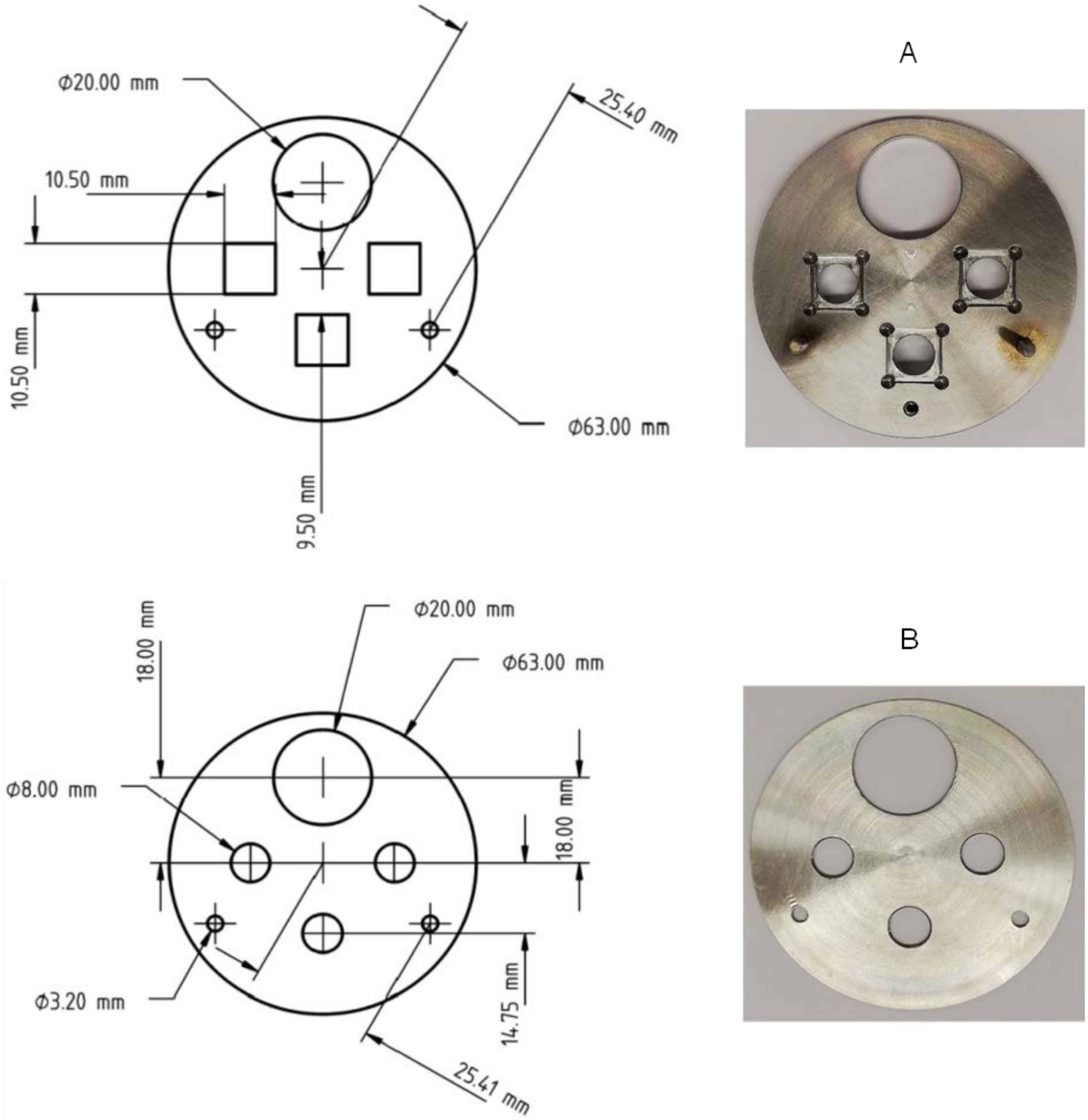

Fig. S3. Schematic representation (left) and images (right) of the substrate support system. The support was used for the sequential or simultaneous deposition processes of perylene and different ionic liquids: ionic liquid/perylene/indium tin oxide (ITO); perylene/ionic liquid/ITO; ionic liquid+perylene/ITO.

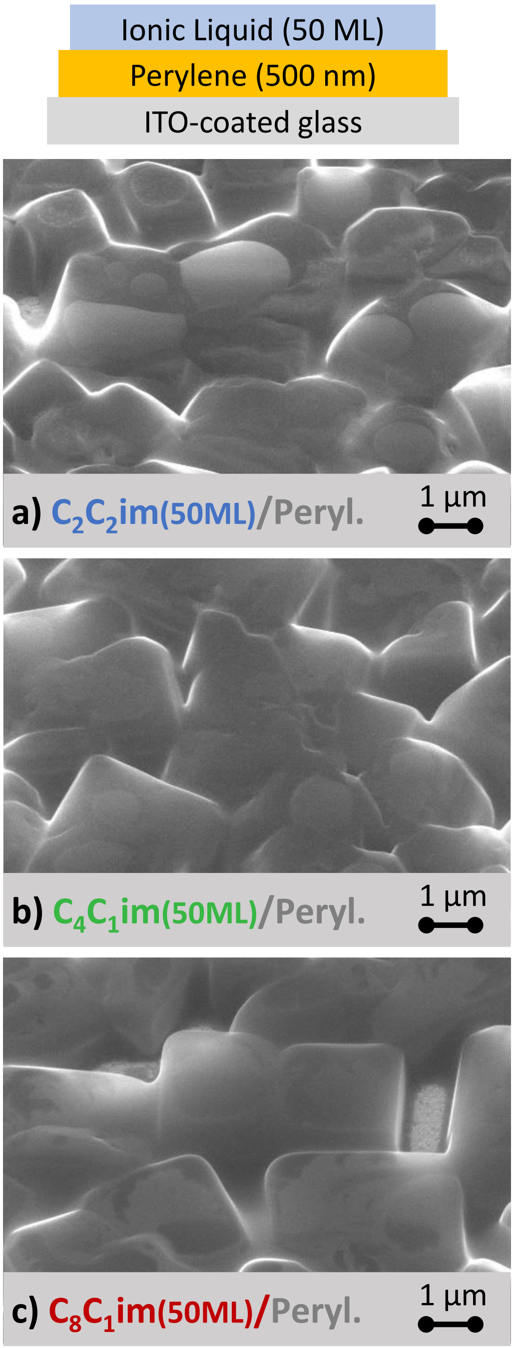

Fig. S4. Detailed morphology of the different microstructures fabricated by sequential PVD of perylene and ionic liquids on ITO-coated glass surfaces [ionic liquid/perylene/ITO]: micrographs of perylene (peryl.) film (500 nm) covered with 50 monolayers (ML) of [C_2C_2im][NTf_2] (a), [C_4C_1im][NTf_2] (b), and [C_8C_1im][NTf_2] (c). Lateral views at 45° were acquired through high-resolution scanning electron microscopy (SEM) by using a secondary electrons detector (SED).

The organic film was found to have good wettability by ionic liquid films. The 3D perylene microstructures seem to be fully covered with a coalesced film (50 ML of thickness) of [C_2C_2im][NTf_2], [C_4C_1im][NTf_2], and [C_8C_1im][NTf_2]. For perylene coated with 50 ML of [C_2C_2im][NTf_2] or [C_4C_1im][NTf_2], the formation of 3D droplets (Figures 2a and 2b) of ILs can be perceived. These results indicate that the first layers of the short-chain alkylimidazolium-based ILs grow two-dimensionally onto the perylene film, followed by the three-dimensional growth of successive layers. A higher percentage of ITO exposed can be perceived for the perylene film coated with 50 ML of [C_8C_1im][NTf_2], which highlights an even higher affinity of the organic film to the long-chain alkylimidazolium cations.

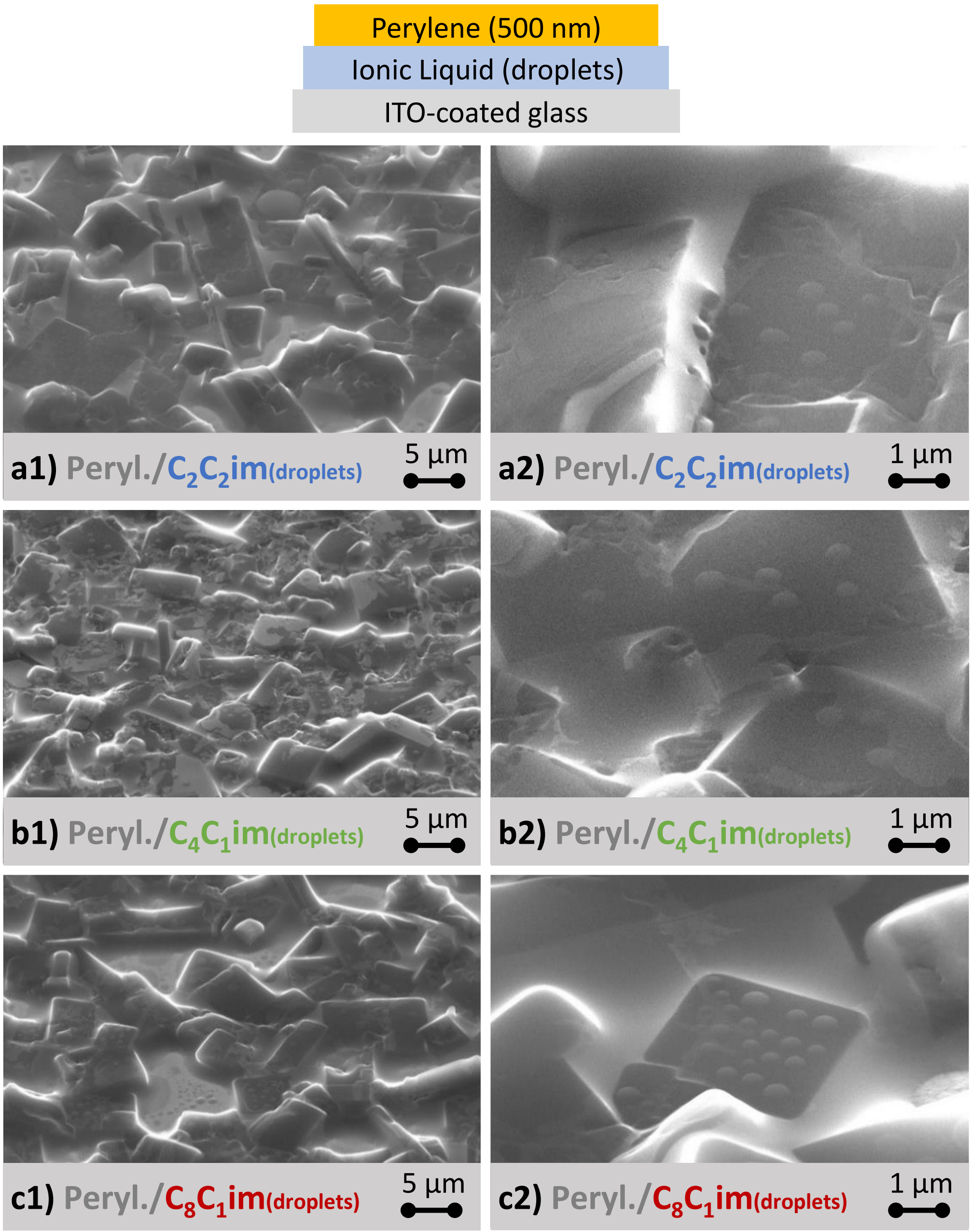

Fig. S5. Detailed morphology of the different microstructures fabricated by inverted sequential PVD of perylene and ionic liquids on ITO-coated glass surfaces [perylene/ionic liquid/ITO]: micrographs of a perylene (peryl.) film deposited onto droplets of [C_2C_2im][NTf_2] (a1,a2), [C_4C_1im][NTf_2] (b1,b2), and [C_8C_1im][NTf_2] (c1,c2). Lateral views at 45° were acquired through high-resolution scanning electron microscopy (SEM) by using a secondary electrons detector (SED). The images obtained at higher magnification (a2, b2, c2) depict the presence of ionic liquid droplets on the top of the perylene crystals. This observation reveals that the perylene molecules might have penetrated inside the droplets where they formed the most stable clusters. As the ITO is a solvophobic surface to the ILs and there is a great interaction between the imidazolium cations and the perylene molecules, the ionic liquid accompanies the growth of the organic film. This effect is highly pronounced for [C_8C_1im][NTf_2].

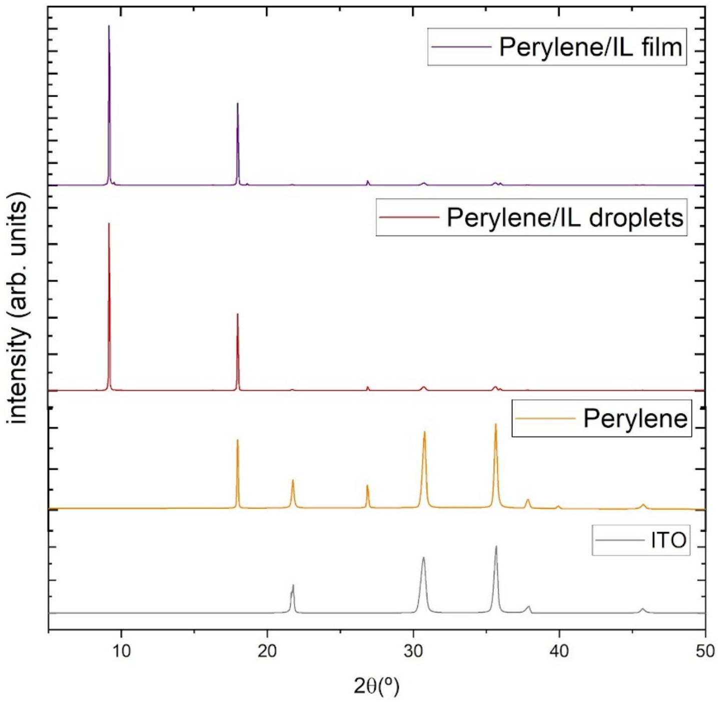

Fig. S6. X-ray diffraction patterns of the ITO substrate, the perylene film, and the perylene film deposited onto droplets (Perylene/IL droplets) or a coalesced film (Perylene/IL film) of $[C_2C_2im][NTf_2]$. The different plots are not scaled to better observe the difference between them.

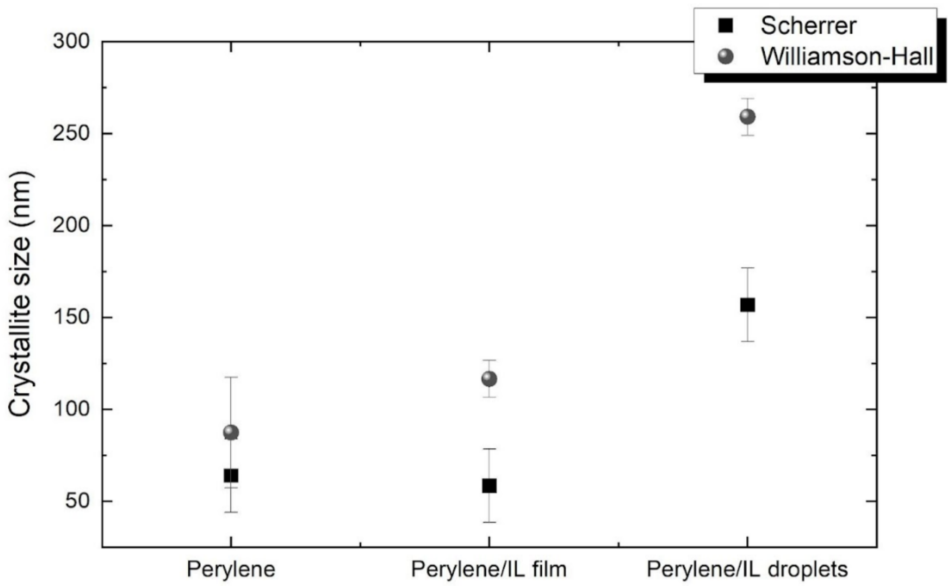

Fig. S7. Predicted crystallite sizes, calculated through Scherrer equation and Williamson-Hall Plot, of the perylene film and the perylene film deposited onto a coalesced film (Perylene/IL film) or onto droplets (Perylene/IL droplets) of $[C_2C_2im][NTf_2]$.

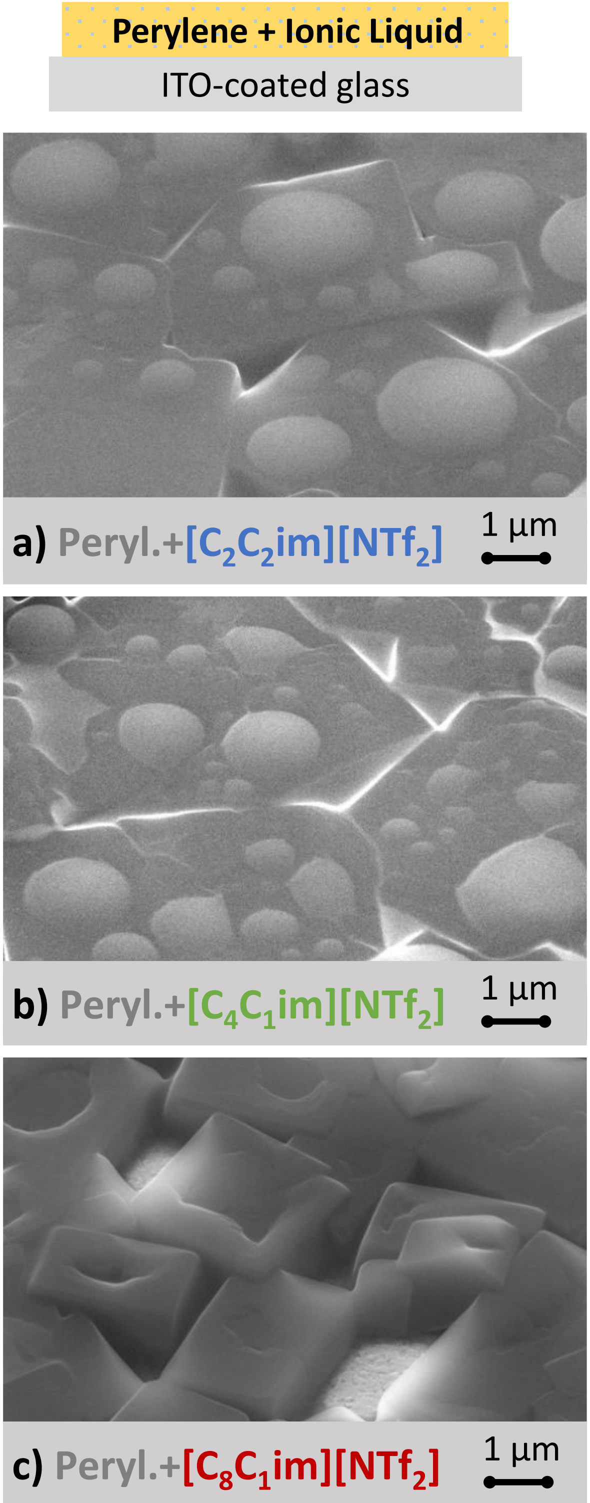

Fig. S8. Detailed morphology of the different microstructures fabricated by simultaneous PVD of perylene and ionic liquids on ITO-coated glass surfaces [(perylene + ionic liquid)/ITO]: micrographs of nanocomposites of perylene (peryl.) and [C_2C_2im][NTf_2] (a), nanocomposites of perylene and [C_4C_1im][NTf_2] (b1), and nanocomposites of perylene and [C_8C_1im][NTf_2] (c). Lateral views at 45° were acquired through high-resolution scanning electron microscopy (SEM) by using a secondary electrons detector (SED).

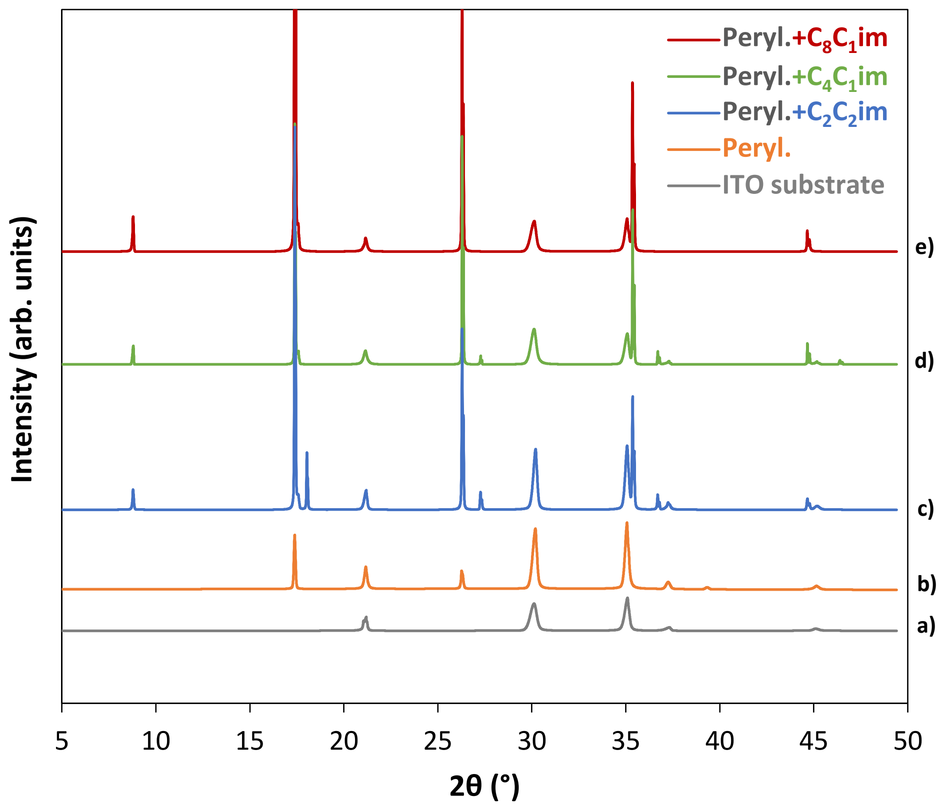

Fig. S9. X-ray diffraction patterns of the ITO substrate (a), the perylene (peryl.) film (b), and the different microstructures/composites fabricated: nanocomposites of perylene and [C_2C_2im][NTf_2] (c); nanocomposites of perylene and [C_4C_1im][NTf_2] (d); nanocomposites of perylene (peryl.) and [C_8C_1im][NTf_2] (e).

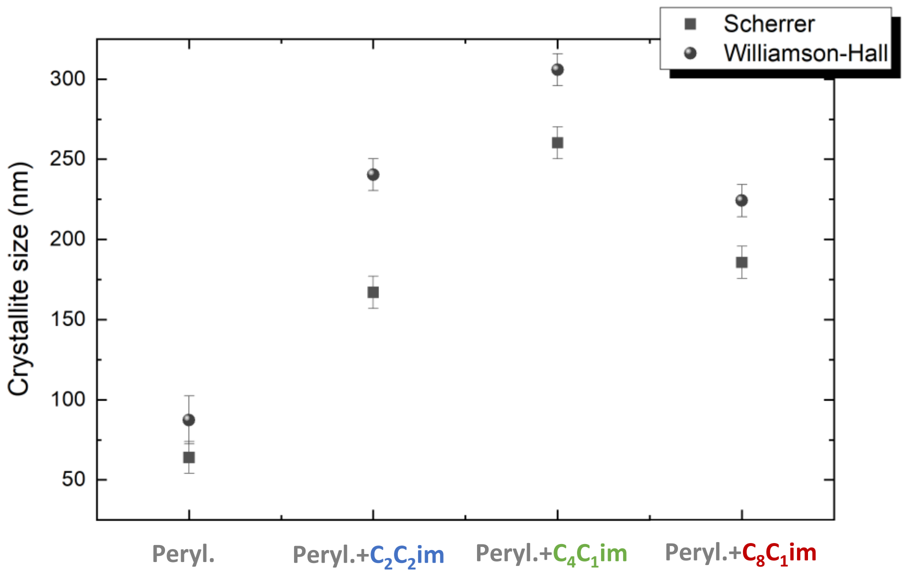

Fig. S10. Predicted crystallite sizes, calculated through Scherrer equation and Williamson-Hall Plot, of the perylene film (Peryl.), the nanocomposites of perylene and [C_2C_2im][NTf_2] (Peryl.+C_2C_2im), the nanocomposites of perylene and [C_4C_1im][NTf_2] (Peryl.+ C_4C_1im), and the nanocomposites of perylene and [C_8C_1im][NTf_2] (Peryl.+ C_8C_1im).

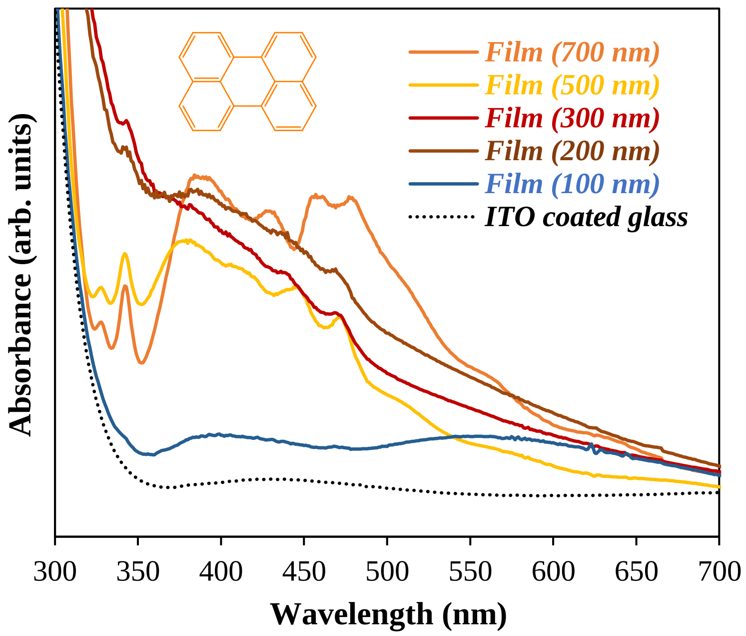

Fig. S11. UV-vis absorption spectra of perylene films (deposited on ITO/glass) with different thicknesses. The spectrum of the ITO-coated glass substrate (ITO/glass) is presented for comparison. These measurements were made in perylene films kept at ambient conditions (inside a box for a long time, > 1 month). As expected, peaks with higher absorbance were observed for the thicker perylene films.

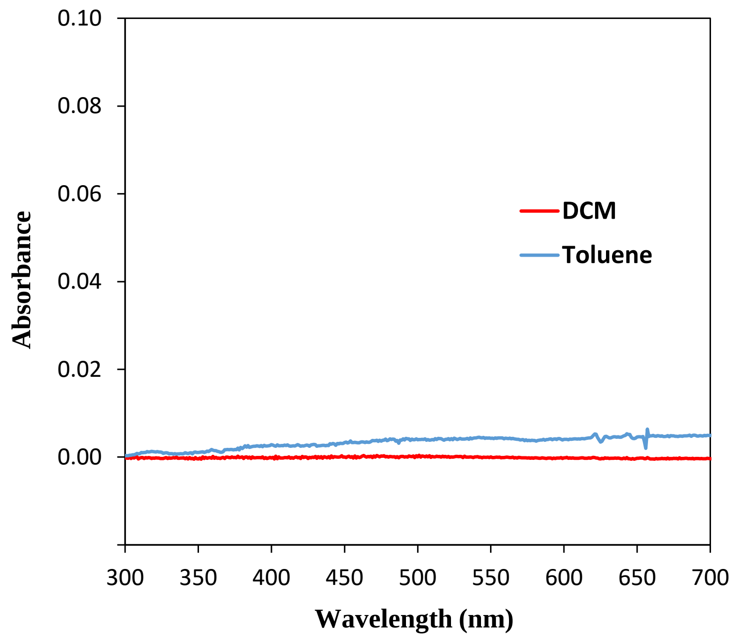

Fig. S12. UV-vis absorption spectra, recorded at T = 298.15 K, of the solution medium (toluene and DCM).

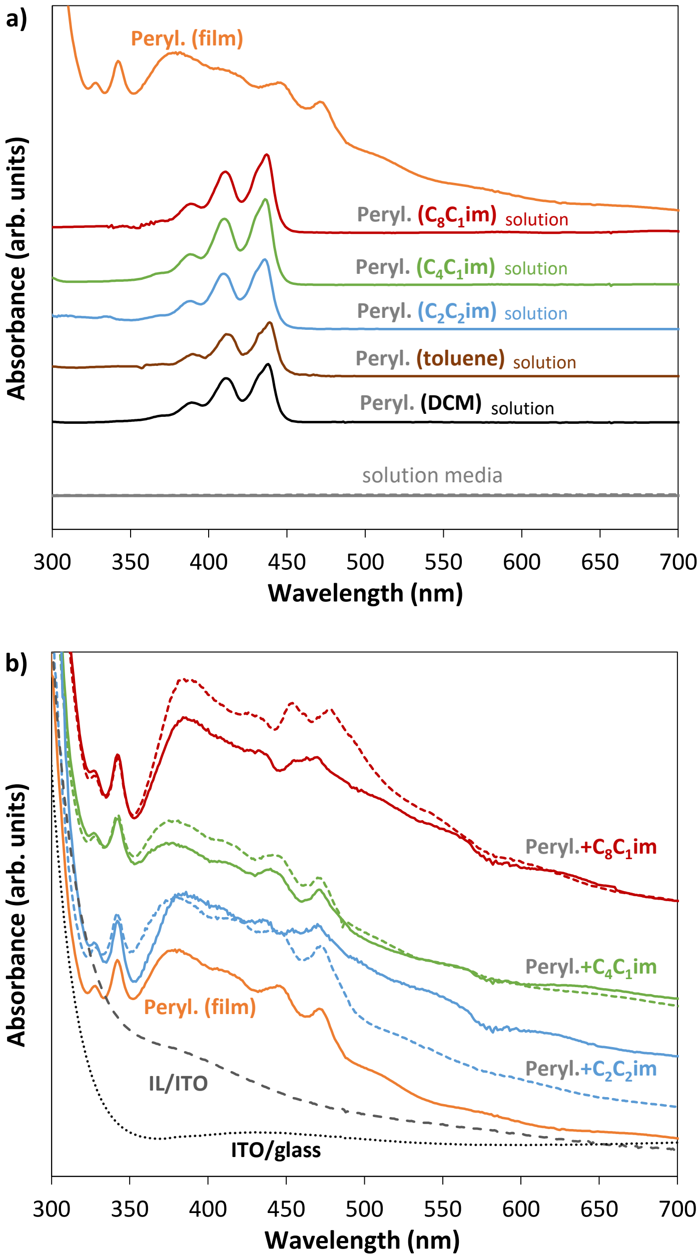

Fig. S13. UV-vis absorption spectra (a), recorded at T = 298.15 K, for solutions of perylene ([peryl.] ≈ 10^{-5} mol·dm^{-3}) obtained by using different solvents: DCM (Peryl. (DCM)); toluene (Peryl. (toluene)); $[C_2C_2im][NTf_2]$ (Peryl. (C_2C_2im)); $[C_4C_1im][NTf_2]$ (Peryl. (C_4C_1im)); $[C_8C_1im][NTf_2]$ (Peryl. (C_8C_1im)). UV-vis absorption spectra (b) of perylene thin films (500 nm of thickness) covered with 400 monolayers (ML) of different ionic liquids (C_8C_1im; C_4C_1im, and C_2C_2im) (solid lines) and spectra of perylene films deposited simultaneously with the same ionic liquids (dashed lines). Spectra of the solution media (DCM and toluene), of a perylene film (Peryl.), the ionic liquid droplets deposited onto ITO (IL/ITO), and the ITO-coated glass substrate (ITO/glass) are presented for comparison.

Table S1. Detailed experimental conditions for the PVD process of the various film architectures: effusion temperature ($T_{eff.}$); equilibrium vapor pressure (*EVP*); mass flow rate at the Knudsen effusion cell orifice (*Φ* (Knudsen cell)); mass flow rate at the substrate surface (*Φ* (QCM)) and corresponding deposition rate in $Å \cdot s^{-1}$; geometric factor; deposition time; thin film thickness (nm or ML, ML = monolayers).

Precursor	$T_{eff.}$	*EVP*	*Φ* (Knudsen cell)	*Φ* (QCM)	Geometric factor	Deposition rate	Deposition time	Thickness
	K	Pa	$\mu g \cdot cm^{-2} \cdot s^{-1}$	$ng \cdot cm^{-2} \cdot s^{-1}$		$Å \cdot s^{-1}$	min	nm or ML
	Sequential deposition: Ionic Liquid (50 or 400 ML) / Perylene (500 nm) | substrate: ITO							
Perylene	443	≈ 0.72	≈ 215	10.9 ± 0.4	5×10^{-5}	0.81 ± 0.03	103	500 nm
$[C_2C_2im][NTf_2]$	478	≈ 0.09	≈ 33	8.1 ± 0.4	2×10^{-4}	0.55 ± 0.03	12	50 ML
$[C_2C_2im][NTf_2]$	478	≈ 0.09	≈ 33	9.6 ± 1.2	3×10^{-4}	0.65 ± 0.08	79	400 ML
$[C_4C_1im][NTf_2]$	483	≈ 0.08	≈ 29	7.5 ± 0.7	3×10^{-4}	0.52 ± 0.05	13	50 ML
$[C_4C_1im][NTf_2]$	483	≈ 0.08	≈ 29	9.1 ± 2.3	3×10^{-4}	0.63 ± 0.16	83	400 ML
$[C_8C_1im][NTf_2]$	498	≈ 0.12	≈ 46	5.1 ± 1.7	1×10^{-4}	0.39 ± 0.13	18	50 ML
$[C_8C_1im][NTf_2]$	498	≈ 0.12	≈ 46	6.2 ± 1.5	1×10^{-4}	0.47 ± 0.11	120	400 ML
	Inverted sequential deposition: Perylene (20, 50 or 500 nm) / Ionic liquid (200 ML) | substrate: ITO							
Perylene	443	≈ 0.72	≈ 215	11.5 ± 0.4	5×10^{-5}	0.85 ± 0.03	4	20 nm
Perylene	443	≈ 0.72	≈ 215	11.1 ± 0.4	5×10^{-5}	0.82 ± 0.03	10	50 nm
Perylene	443	≈ 0.72	≈ 215	11.6 ± 0.4	5×10^{-5}	0.86 ± 0.03	97	500 nm
$[C_2C_2im][NTf_2]$	478	≈ 0.09	≈ 33	6.2 ± 2.2	2×10^{-4}	0.42 ± 0.15	61	200 ML
$[C_4C_1im][NTf_2]$	483	≈ 0.08	≈ 29	7.1 ± 1.3	2×10^{-4}	0.49 ± 0.09	53	200 ML
$[C_8C_1im][NTf_2]$	498	≈ 0.12	≈ 46	5.5 ± 0.4	1×10^{-4}	0.42 ± 0.03	67	200 ML
	Simultaneous deposition: Perylene + Ionic liquid (≈ 500 nm) | substrate: ITO							
Perylene	443	≈ 0.72	≈ 215	14.9 ± 1.6		1.1 ± 0.1	76	≈ 500 nm
$[C_2C_2im][NTf_2]$	478	≈ 0.09	≈ 33					
Perylene	443	≈ 0.72	≈ 215	13.9 ± 2.0		1.0 ± 0.2	81	≈ 500 nm
$[C_4C_1im][NTf_2]$	483	≈ 0.08	≈ 29					
Perylene	443	≈ 0.72	≈ 215	16.2 ± 1.8		1.2 ± 0.1	69	≈ 500 nm
$[C_8C_1im][NTf_2]$	498	≈ 0.12	≈ 46					